Design of Single-Input-Single-Output Compliant Mechanisms for Practical Applications Using Selection Maps

Sudarshan Hegde
e-mail: hegde@mecheng.iisc.ernet.in

G. K. Ananthasuresh
e-mail: suresh@mecheng.iisc.ernet.in

Mechanical Engineering,
Indian Institute of Science,
Bangalore 560012, India

We present an interactive map-based technique for designing single-input-single-output compliant mechanisms that meet the requirements of practical applications. Our map juxtaposes user-specifications with the attributes of real compliant mechanisms stored in a database so that not only the practical feasibility of the specifications can be discerned quickly but also modifications can be done interactively to the existing compliant mechanisms. The practical utility of the method presented here exceeds that of shape and size optimizations because it accounts for manufacturing considerations, stress limits, and material selection. The premise for the method is the spring-leverage (SL) model, which characterizes the kinematic and elastostatic behavior of compliant mechanisms with only three SL constants. The user-specifications are met interactively using the beam-based 2D models of compliant mechanisms by changing their attributes such as: (i) overall size in two planar orthogonal directions, separately and together, (ii) uniform resizing of the in-plane widths of all the beam elements, (iii) uniform resizing of the out-of-plane thicknesses of the beam elements, and (iv) the material. We present a design software program with a graphical user interface for interactive design. A case-study that describes the design procedure in detail is also presented while additional case-studies are posted on a website. [DOI: 10.1115/1.4001877]

Keywords: compliant mechanisms, spring-leverage model, selection map

1 Introduction

In this paper, we present a design technique for single-input-single-output compliant mechanisms in view of practical applications. Our method is based on selection from an existing set of compliant mechanisms and modifying them to suit the practical requirements of a new problem. Our approach resembles Ashby's method of material selection from a database [1]. Just as relevant properties of materials are used to create a map of existing materials in Ashby's method, in this paper, relevant characteristics of existing compliant mechanisms are used to create a map and show on it a feasible map that satisfies the user-specifications. The compliant mechanisms in the database are already manufactured and some are used in real applications.

The development of systematic design techniques has been an active area of research in the field of compliant mechanisms. Two such techniques are the pseudo-rigid-body model-based design (Refs. [2,3]) and the topology optimization approach (Refs. [4,5] and references therein cover a wide body of literature on topology optimization with gradient-based continuous optimization algorithms while Ref. [6] uses genetic algorithms). In the pseudo-rigid-body approach, topology and the type of linkage, i.e., the number of links and their connectivity are usually assumed. It is also difficult to automate this method. In contrast, the topology optimization method requires minimal user intervention. Two open-access software programs—TOPOPT (www.topopt.dtu.dk) and YINSYN (www.mecheng.iisc.ernet.in/~suresh/YinSyn)—that use the topology optimization method are currently available.

Both the abovementioned methods are fairly sophisticated and require good understanding of kinematics, elastic deformation analysis, and optimization in order to implement and use them. In this work, we take an approach toward the design of compliant mechanisms that is suitable even for a novice user who is not familiar with the compliant mechanism theory. The method involves the user in the design process. It is based on the selection among known designs, most of which were produced by topology optimization but some were conceived intuitively. We do this for two reasons: (i) the number of compliant mechanisms in use for practical applications is steadily growing and there is a large enough set of these mechanisms [7] to choose from and (ii) all practical requirements cannot be easily incorporated into the topology optimization or the pseudo-rigid-body approach at the current stage of their development.

An additional benefit of the method presented in this paper is that, unlike in other methods, it is possible to know if the specifications of a practical problem have a solution or not before it is solved. This is made possible by representing the user-specified practical requirements and the kinematic and elastostatic features of real compliant mechanisms in the database, simultaneously, on a 2D map. Thus, the methodology presented here allows the user to see on a 2D map how different existing compliant mechanisms fare against the requirements of his/her practical application. The map then aids in selecting a suitable mechanism and, if necessary, modifying it for that application. A graphical user interface (GUI) is developed to aid the interaction. The interactive procedure is quite rapid and the computation involved is not much, and hence it yields mechanisms that satisfy the user-specifications within a few minutes.

The basis for the simultaneous representation of the practical requirements and the suitability of the existing mechanisms on a 2D map is the characterization of a compliant mechanism by only three lumped spring-leverage (SL) model constants (see Refs. [7,8]). The SL model is explained in Sec. 2. The selection methodology is explained in Sec. 3. The features of the GUI are de-

Contributed by the Mechanisms and Robotics Committee of ASME for publication in the JOURNAL OF MECHANICAL DESIGN. Manuscript received October 20, 2009; final manuscript received May 13, 2010; published online August 13, 2010. Assoc. Editor: Mary Frecker.

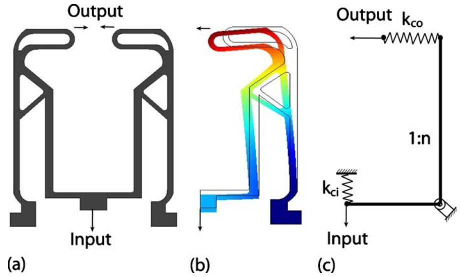

Fig. 1 Spring-leverage model: (*a*) a compliant gripper, (*b*) its symmetric half used in deformation analysis, and (*c*) its representation as a lever with geometric amplification factor *n*, the input-side spring stiffness k_{ci}, and the output side spring stiffness k_{co}

scribed in Sec. 4 using a case-study that illustrates the use of our approach with a real practical problem. The design software and additional case-studies can be accessed at a website (www.mecheng.iisc.ernet.in/~hegde/paper). Main points of the paper, current limitations of the method and future extensions are noted in Sec. 5.

2 SL Model

The kinematics and the elastic deformation of the single-input-single-output compliant mechanisms can be expressed by the SL model to account for its displacement-amplifying and force-transmission features [7]. The concept of the SL model is similar to representing the static behavior of an elastic structure by a single spring. However, the compliant mechanism under consideration here has two ports of significance: the input port and the output port. The input port is where the input force or input displacement is applied and the output port is where the output force or the output displacement is desired. A compliant mechanism has different stiffnesses at input and output ports. Consequently, two springs are introduced at the input and the output ports with the *input port spring stiffness* k_{ci} and the *output port spring stiffness* k_{co}. In order to account for the amplification between the input and the output, a lever is introduced between the two springs. See Fig. 1. Sometimes, as shown in Fig. 2, an inverting mechanism may be needed to reverse the direction of the lever on the output side to match the desired output direction.

The lever in Fig. 1 and the leverage mechanism of Fig. 2 are only symbolic but they can also be designed to match the kinematic behavior of the compliant mechanism. The important feature is the amplification of the lever, called the *inherent geometric amplification factor n*, of the mechanism. Thus, as shown in Figs. 1 and 2, the compliant mechanism is replaced by a lever or a leverage that has finite stiffnesses at the input side as well as at the output side.

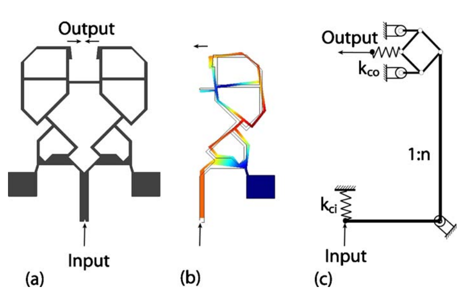

Fig. 2 SL model to match the kinematic behavior: (*a*) a compliant gripper, (*b*) its symmetric half used in deformation analysis, and (*c*) a leveraging mechanism to revert the direction of motion from input to output in the SL model to match the output direction in the gripper

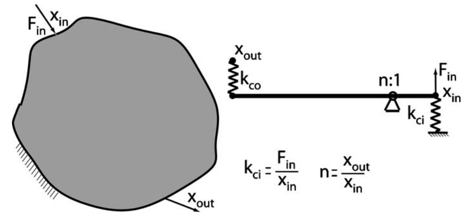

Fig. 3 The first load case used to find the input-side stiffness k_{ci} and the inherent geometric amplification factor *n* of the SL model

It can be seen that the aforementioned lumped model can also explain the following fact observed in compliant mechanisms: the de-amplification of the motion from the output to the input is not the reciprocal of amplification from the input to the output. It should also be noted that when the SL constants of two compliant mechanisms are the same, they both behave in exactly the same way as far as the single-input-single-output application is concerned under static equilibrium conditions. The method of computing the SL constants is explained next.

2.1 Determining the SL Constants. In order to compute the SL constants, we need to do two deformation analyses of the compliant mechanism under two different load cases. In the first load case, we apply an input force $F_{\rm in}$ only and measure the displacement $x_{\rm in}$ at the input (see Fig. 3). With these, as in an ordinary lumped spring modeling of an elastic structure, we compute the input-side stiffness k_{ci}.

$$k_{ci} = \frac{F_{\rm in}}{x_{\rm in}} \tag{1}$$

By also measuring the output displacement $x_{\rm out}$, we compute the inherent amplification n.

$$n = \frac{x_{\rm out}}{x_{\rm in}} \tag{2}$$

Next, we consider a different loading condition, as shown in Fig. 4, to get k_{co}. Here, the force $F_{\rm out}$ is applied only at the output to measure the resulting displacement at the input $y_{\rm in}$ and at the output $y_{\rm out}$. By applying static equilibrium to the SL model in Fig. 4, an expression for k_{co} is calculated as follows.

$$k_{co} = \frac{F_{\rm out}}{y_{\rm out} - n y_{\rm in}} \tag{3}$$

3 Selection and Redesign Methodology

The selection and redesign methodology consists of three steps. The first involves representing the requirements of the practical application as a 2D map. The second step consists of representing the existing compliant mechanisms in the database on the same map. If at least one of the mechanisms lies inside the feasible map with the appropriate geometric amplification and the designer is satisfied with it, the method ends there. Otherwise, it continues

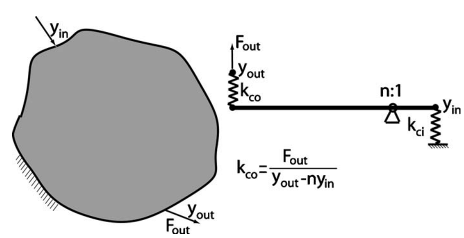

Fig. 4 The second load case used to find the output side spring stiffness k_{co} of the SL model

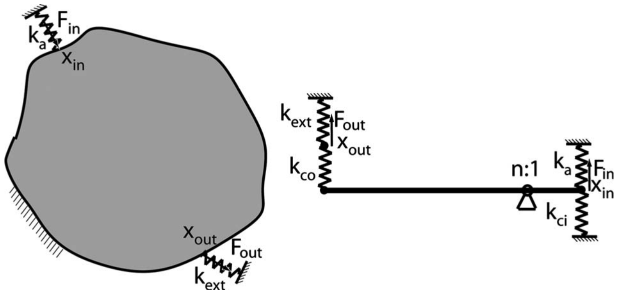

Fig. 5 The variables involved in the SL model of a single-input-single-output compliant mechanism

with the selection of the mechanism(s) that is (are) closest to the feasible map. The third step is the process of redesign of the selected mechanism so that the modified mechanism satisfies the user-specifications. These are explained next.

3.1 Plotting the Practical Requirements on a Map. The variables involved in specifying the practical intent of a single-input-single-output compliant mechanism are listed below.

(i) input force: $F_{\text{in}L} \leq F_{\text{in}} \leq F_{\text{in}H}$
(ii) input displacement: $x_{\text{in}L} \leq x_{\text{in}} \leq x_{\text{in}H}$
(iii) output load: $F_{\text{out}L} \leq F_{\text{out}} \leq F_{\text{out}H}$
(iv) output displacement: $x_{\text{out}L} \leq x_{\text{out}} \leq x_{\text{out}H}$
(v) actuator's stiffness (assumed to be linear) at the input: $k_{aL} \leq k_a \leq k_{aH}$
(vi) external stiffness (assumed to be linear) at the output: $k_{\text{ext}L} \leq k_{\text{ext}} \leq k_{\text{ext}H}$

A designer is usually interested in specifying the lower and upper bounds (maximum and minimum values denoted by subscripts H and L, respectively) on the specification variables rather than a particular value. However, if the user intends to specify a single value to a specification variable, the two bounds can be specified to be equal.

The first step is to identify the range of values of the SL constants that can meet the user-specifications. Toward this, we begin with the potential energy of the SL model shown in Fig. 5:

$$PE = \frac{1}{2}k_{ci}x_{\text{in}}^2 + \frac{1}{2}k_{co}(x_{\text{out}} - nx_{\text{in}})^2 + \frac{1}{2}k_{\text{ext}}x_{\text{out}}^2 + \frac{1}{2}k_a x_{\text{in}}^2 - F_{\text{out}}x_{\text{out}} - F_{\text{in}}x_{\text{in}} \tag{4}$$

Note that the potential energy is the sum of the strain energy and the negative of the work done by the external forces.

By differentiating PE with respect to x_{in} and x_{out}, and equating them to zero, we get two static equilibrium equations, the rearrangement of which gives the expressions for k_{ci} and k_{co} in terms of the specification variables and n.

$$k_{ci} = \frac{F_{\text{in}} - nk_{\text{ext}}x_{\text{out}} + nF_{\text{out}} - k_a x_{\text{in}}}{x_{\text{in}}} \tag{5}$$

$$k_{co} = \frac{F_{\text{out}} - k_{\text{ext}}x_{\text{out}}}{x_{\text{out}} - nx_{\text{in}}} \tag{6}$$

It can be verified that k_{ci} and k_{co}, given in Eqs. (1) and (3), are special cases of Eqs. (5) and (6) under the load cases shown in Figs. 3 and 4.

The task now is to investigate, which values of the six specification variables and n lead to realistic (i.e., positive and not too large or too small) values of k_{ci} and k_{co}. This implies that we need to solve Eqs. (5) and (6) along with 12 inequalities corresponding to the lower and upper bounds on the six specification variables. Note that n can take either a positive or negative value. Although it is possible to compute the complete set of feasible values of k_{ci} and k_{co}, which defines the *feasible map* for the user-specifications, in this paper, we follow a simple approach to obtain a subset of the feasible map as described next.

Equations (5) and (6) help us draw a curve with lower specifications on a k_{ci}-k_{co} map by varying n while fixing all the specification variables at their lower specification values. The value of n that makes k_{co} of Eq. (6) negative, forms the lower limit of n. The upper limit of n is taken to be 50 or n that leads to a negative k_{ci} in Eq. (6), whichever is lower. See Fig. 6(*a*). Thus, the points on this curve and the corresponding value of n satisfy Eqs. (5) and (6) with the lower bounds of the specification variables. Similarly, the curve of upper specifications can be drawn using the upper bounds on the specification variables and varying n. Several such curves can be drawn, which lie between the lower and the upper specifications-curves by varying the six specified variables uni-

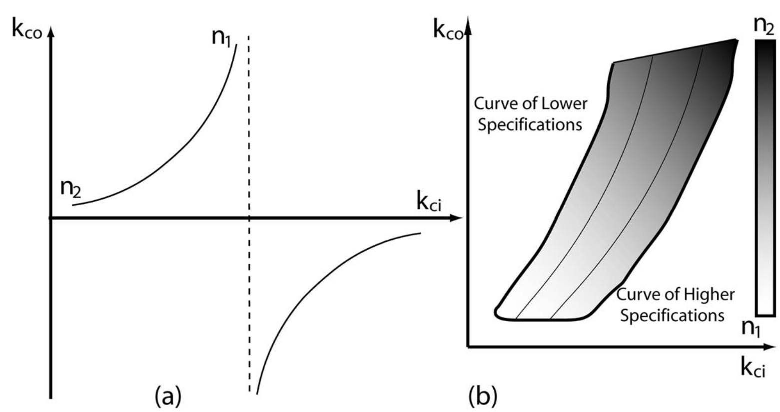

Fig. 6 Drawing the feasible map on the selection map: (*a*) the points on the curve are generated for lower bounds of the specification variables but with different values of *n*; only the part of the curve corresponding to the positive values of k_{ci} and k_{co} is considered and (*b*) the feasible map is bounded by the curves corresponding to the upper and lower specification variables and is filled with a gray color scale based on the value of *n*

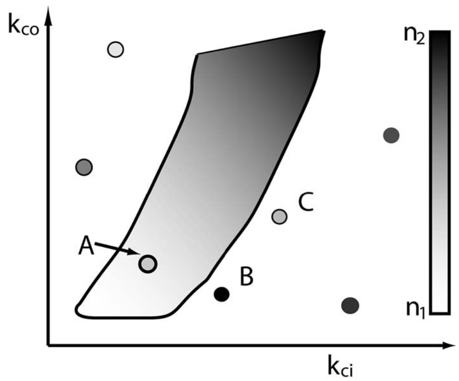

Fig. 7 The dots represent the compliant mechanisms in the database

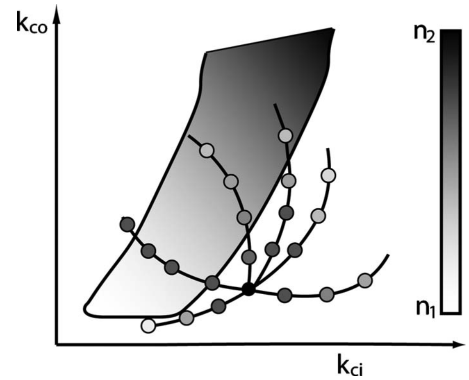

Fig. 8 The six parameter curves from a selected mechanism, which is the mechanism closest to the feasible map

formly between the lower and the upper bounds (see Fig. 6(*b*)).

The region bounded by the upper and lower specifications curves is a subset of the feasible map of k_{ci} and k_{co} that satisfies user-specifications. The actual feasible map is much larger than the region bounded between the lower and upper specification curves. However, for simplicity, we use only a subset in this paper, as noted above.

For each point (k_{ci}, k_{co}) within the feasible map, there is at least one set of values of specification variables and a corresponding value of n. We color the feasible map on a gray scale with the gray scale value at each point corresponding to the value of n at that point, as shown in Fig. 6(*b*).

If the feasible map is null, it immediately follows that user-specifications are impractical. Similarly, if the feasible map is too small, it would imply that the specifications are stringent. Such a judgment is not possible in the usual topology, shape, and size optimizations. This is a distinguishing feature of the approach presented in this paper. Next, we show how existing compliant mechanisms can be shown on the k_{ci} and k_{co} map so that they can either be readily selected or modified.

3.2 Plotting the Mechanisms on the k_{ci}-k_{co} Map and Selecting the Mechanism. Each compliant mechanism in the database can be represented on the k_{ci}-k_{co} map as a dot, as shown in Fig. 7. The location of the dot corresponds to the values of k_{ci} and k_{co} while the gray scale value of the fill color of the dot indicates the value of n of the mechanism (denoted by n_m from here onward). Therefore, when the colored dot corresponding to a compliant mechanism lies within the feasible map and its n_m matches the n value of the map (denoted with n_s from here onward), then we can conclude that that mechanism meets the user's requirements. If so, the user can readily select such a mechanism. Dot A in Fig. 7 is such a point. But this happens rarely unless the database is extensive, which is not the case at present. Hence, the user needs to redesign some likely candidates (e.g., dots B and C) that are not within the feasible map with a matching gray scale value but are sufficiently close. If the user has some functional requirements such as the positions/directions of the input and output or the orientation of the mechanism, then the user selects the mechanism topology that can satisfy the functional intent for redesign. The process of redesign is explained next.

3.3 Redesigning With Parameter Curves On the k_{ci}-k_{co} Map. An initially infeasible mechanism of the database can be modified by changing some or all of its parameters, which are a set of size and shape variables as well as the material of the mechanism. The size of the mechanism is changed by uniform increase or decrease in the in-plane width or the out-of-plane thickness of the beam members. In other words, the ratios of the in-plane widths of the different members of the selected mechanism remain the same even after the modification. The shape and size of the mechanism are changed in the following three ways: (a) the *X*-coordinates of the nodes of the beam element in the meshed model are uniformly changed, (b) the *Y*-coordinates of the nodes of the meshed model are uniformly changed, and (c) both the coordinates of the nodes are changed uniformly. Additionally, the user can also change the material of the selected mechanism. Thus, parameters of the compliant mechanism that can be changed are as follows:

i. resizing the mechanism only in the x-direction
ii. resizing the mechanism only in the y-direction
iii. resizing the mechanism in both the directions at a chosen aspect ratio
iv. uniformly changing the in-plane widths of all the beam elements
v. uniformly changing the out-of-plane thicknesses of all the beam elements
vi. changing the material of the mechanism

Figure 8 shows how an infeasible dot may be brought into the feasible map by changing the values of one or more of the six parameters. Each parameter curve in Fig. 8 indicates how the k_{ci} and k_{co} of the mechanism change as that particular parameter is increased or decreased from its current value. Note that not all curves tend toward the feasible map. Indeed, the user can readily see which parameters, if changed, can make the mechanism feasible for his/her specifications. This is useful for interactive redesign of the mechanisms in the database.

By entering into the feasible map by following a parameter curve with a matching gray scale fill color of n_m with that of n_s, the user can obtain a feasible mechanism and save it. This possibility is shown in Fig. 9.

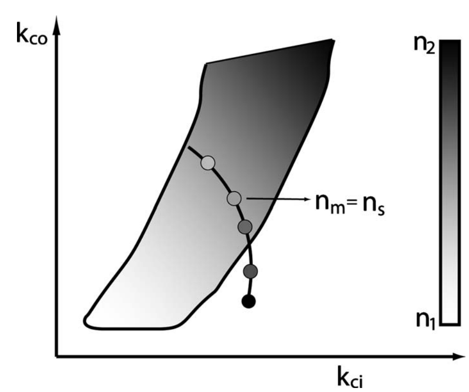

Fig. 9 One of the curves is selected for design. Note that there is a matching of n_m with n_s along this curve.

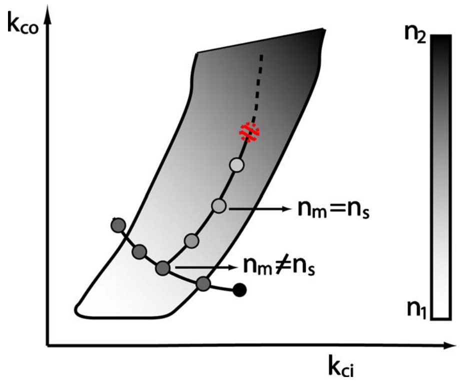

Fig. 10 Redesign by using multiple parameter curves. One of the curves is selected for redesign but it does not result in matched values of n_m and n_s. Hence, an alternate parameter curve is pursued from within the feasible map to obtain a feasible mechanism. The red STOP sign on the second parametric curve indicates that a particular manufacturing process limit has been reached because of the change in the corresponding parameter.

Figure 10 shows a situation where the feasible map can be entered along a parameter curve but n_m and n_s cannot be matched. When this happens, the other parameter curves can be pursued from inside the feasible map, as illustrated in Fig. 10. In the GUI, which is described later, the user can see the mechanism and its animation as it is changed. If the user is not satisfied with size, the manufacturability, orientation or any other aspect of the redesigned mechanism, he/she may choose the next mechanism closest to the feasible map and repeat the process. This interactive procedure is quite fast. The user stops after sufficient number of feasible mechanisms are found. This number may be just one or many—usually many are possible.

Instead of the interactive redesign procedure described above, one may consider solving a traditional shape and/or size optimization problem in terms of the six parameters. Such a problem will have nonlinear constraints in terms of these parameters to ensure feasible values for k_{ci} and k_{co} as per Eqs. (5) and (6). Furthermore, the user would need to choose particular values of the specification variables rather than giving a range for each of them. This is not only restrictive but it is also more time-consuming than the interactive procedure. Furthermore, manufacturing considerations on features such as minimum/maximum width, thickness, or gap are harder to implement in size and shape optimizations. On the other hand, in GUI-driven interactive redesign, the user can select a manufacturing process whose limitations can be readily brought into the procedure, as explained next.

3.4 Including the Manufacturing Process Constraints. Let us suppose that the mechanism shown in Fig. 11(*a*) is selected because it is closest to the feasible map. Let us also suppose that

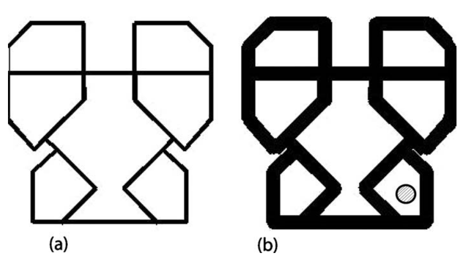

Fig. 11 Redesigning a mechanism by changing its in-plane width: (*a*) the mechanism as it is in the database and (*b*) redesigned mechanism with increased width, which is limited by the tool diameter shown as a hatched circle

computer numerical control (CNC) milling is used to make this mechanism. If the user decides to increase the in-plane width of this mechanism, it is possible to guide the user by indicating the minimum gap limit of CNC milling. As shown in Fig. 11(*b*), the diameter of the mill (the hatched circle) can be checked against the gap between different beams as their widths are increased. This information can be conveyed to the user, as shown in Fig. 10, wherein a STOP sign is displayed along the parameter curve. On the other hand, if the user decides to decrease the width, then the minimum width constraint can also be displayed. Similarly, for other processes also, the limits for various geometric features and the overall size of the mechanism can be handled based on the information provided by the user about the chosen manufacturing process. This important and pragmatic feature is further explained in the next section where the details of GUI are presented.

Furthermore, it is also possible to partition and color the entire k_{ci} and k_{co} graph region as per different manufacturing processes for a chosen mechanism in view of the respective limits of those processes. This allows the user to get a quick view of the relevant manufacturing options and hence exercise that choice in selecting the mechanism and in redesigning it interactively.

4 GUI and a Case Study

Since the design process benefits from the interaction with the user, a GUI (Fig. 12) is developed in MATLAB and JAVA. The GUI is made up of a plot area and a number of panels. In the *specifications* panel, the user enters the values of the lower and upper bounds for the six specification variables. The *show and select* panel can be used to display the feasible map and various mechanisms in the database. The *manufacturing process* panel allows for selecting the manufacturing processes. It also allows the input of minimum gap feature, minimum width feature, minimum and maximum thickness, minimum and maximum sizes that are specific to the selected manufacturing process. The *draw parameter curves* panel can be used to select one, many, or all of the parameter curves for the purpose of drawing them on the graph. The *data-cursor* icon allows the user to select a parameter curve to move the current dot into the feasible map. As the user is following the curve, he/she can see the difference between N_m and N_s, and also the changing attributes of the mechanism in the *current state* panel, in real-time. The GUI automatically places a green dot on the parameter curve when there is a matching between N_m and N_s. The *maximum stress* button can be used to get the maximum stress in the mechanism. The GUI has a provision to save the modified mechanism into a *checkout-bin*, which could be used by the user for the final selection of the mechanism.

We used the GUI to solve a number of practical problems of interest. For brevity, we discuss in detail only one of them here. Additional case-studies are available at a website (www.mecheng.iisc.ernet.in/~hegde/paper).

4.1 Amplifying Mechanism for a Piezoelectric Actuator. Piezoelectric actuators produce large forces but have very small displacements. The design problem, as shown in Fig. 13, is to amplify the motion of a piezoelectric actuator against a specified load.

The characteristics of a piezoelectric actuator are taken as follows. It has a stiffness of 7.5 N/μm, a blocking force of 800 N, and an output stroke of 100 μm. The requirement here is that the displacement at the output should be 300 μm against a load of 200 N. Since, the output stroke of the actuator is 100 μm, the compliant mechanism will be designed for an input displacement of 90 μm.

4.1.1 Plotting the Requirements on the k_{ci}-k_{co} Map. The specifications are tabulated in Table 1. Since the external spring is absent here, the values corresponding to its stiffness are both zero.

As can be seen in Fig. 14, k_{ci}-k_{co} map is infeasible because k_{ci} is negative. Thus, the feasible map for these specifications is null.

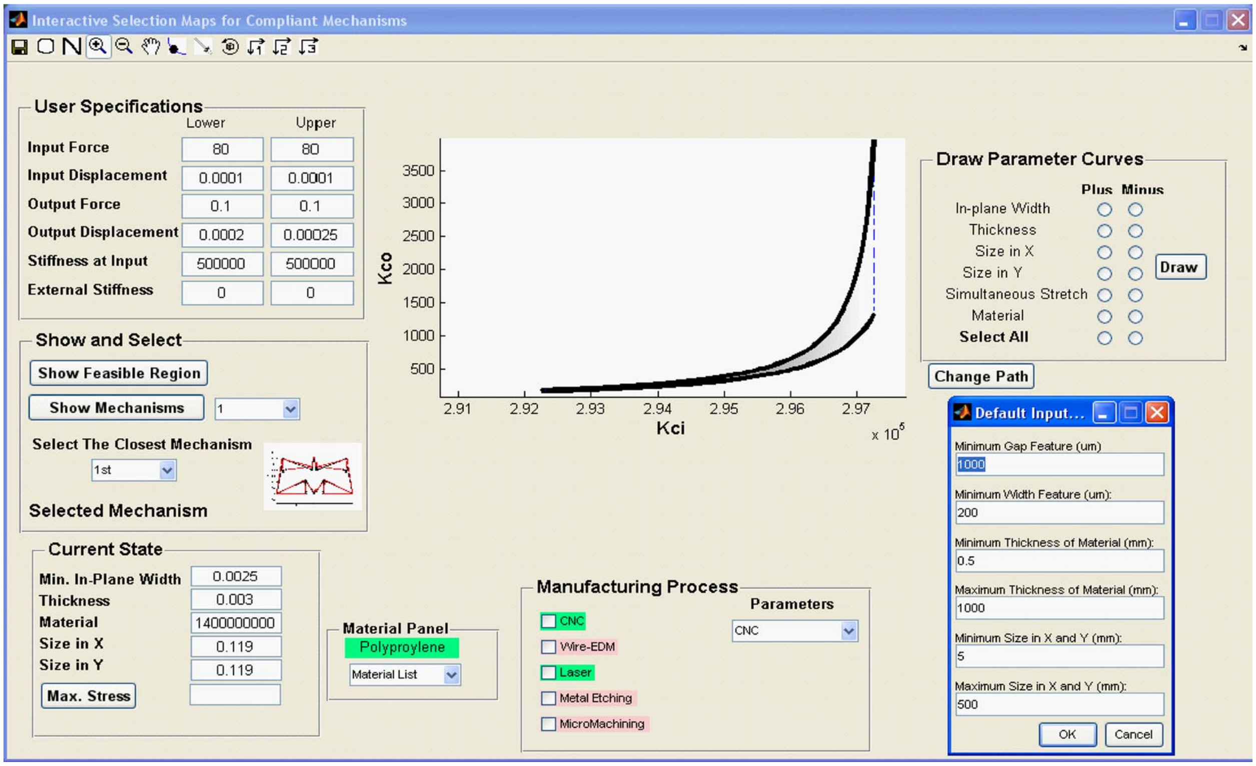

Fig. 12 The graphical user interface, developed using MATLAB, aids in selection and design

This is a case wherein before designing or selecting a mechanism, one can conclude that the requirements of the user are not possible to be met by any mechanism. Knowing that a set of specifications are impossible before designing is an advantage of our approach.

Since the requirements shown in Table 1 are too stringent, we relax them to create some feasible space. Since the characteristics of the piezoactuator cannot be changed, the output load or the output displacement can be relaxed. When the output load requirement is relaxed to 10 N, the feasible map lies in the positive quadrant of k_{ci}-k_{co} axes, which is shown in Fig. 15.

4.1.2 Plotting the Mechanisms on the Map and Selecting the Mechanism for Redesign. Figure 15 shows five mechanisms that are closest to the feasible map. The mechanisms that are not seen in this figure are very far from the feasible map and hence they are far from meeting the user's requirements. The closest mechanism is selected for redesign.

4.1.3 Redesign Using Parameter Curves. Figure 16(*a*) shows the curves emanating from the dot representing the selected mechanism. The red curves indicate the changes in k_{ci} and k_{co} of the designed mechanism when the individual parameters are increased from their present values. The black curves indicate changes in k_{ci} and k_{co} of the designed mechanism when the parameters are decreased from their present values. The legend in Fig. 16(*b*) shows the name of the curve. For example, the width +line indicates the manner in which k_{ci} and k_{co} change when the in-plane width is increased progressively from the current width

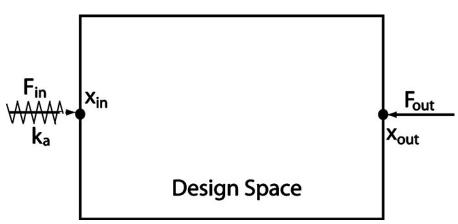

Fig. 13 Design problem of a compliant mechanism to amplify the motion of a piezoelectric actuator at the output

Table 1 Specifications entered by a user

Specification variables	Min	Max
F_{in} (N)	800	800
x_{in} (m)	90×10^{-6}	90×10^{-6}
F_{out} (N)	200	200
x_{out} (m)	290×10^{-6}	310×10^{-6}
k_a (N/m)	7.5×10^{6}	7.5×10^{6}
k_{ext} (N/m)	0	0

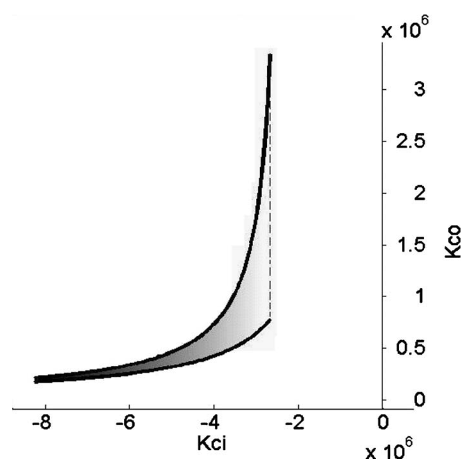

Fig. 14 The feasible map is bound by the curves representing the lower and upper bounds on specification variables

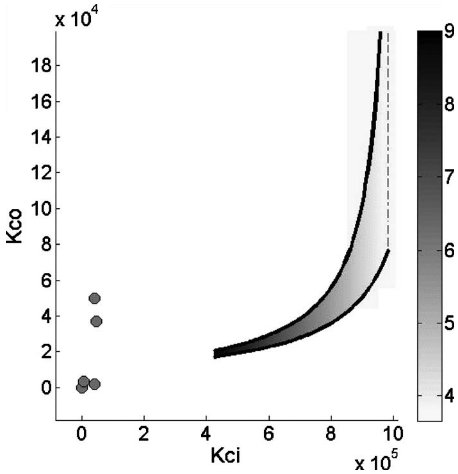

Fig. 15 The feasible map for the modified specifications shown in Table 1 with output load reduced to 10 N. The dots show the mechanisms that are closest to the feasible map.

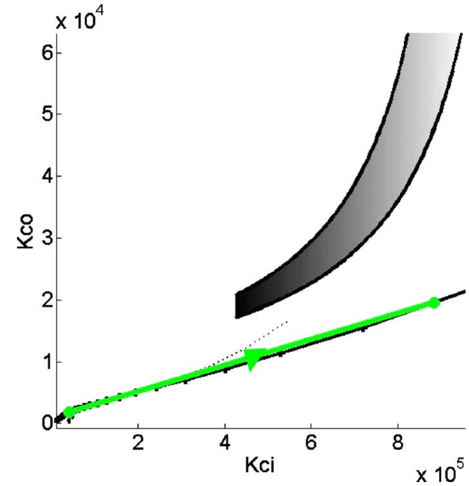

Fig. 17 The *stretchXY*-line is followed up to a certain distance shown by green line at the end of which the change of path option is exercised

with all the other parameters of the mechanism remaining the same. The other curves can be interpreted in a similar way.

4.1.4 Moving the Current Dot Into the Feasible Map. The objective of the redesign is to move the current dot on the map into the feasible map using one of the six parameter curves. This is achieved in a few steps, which is discussed next.

As observed in Fig. 16(*a*), at the outset, none of the curves pass through the feasible map. With a view to move into the feasible map, *stretchXY*-curve is selected and is followed only up to a certain distance indicated by the green line (see Fig. 17). At the end of the green line, a *change path* option is exercised. The curves emanating from this new point of design are shown in Fig. 18. None of the curves except one curve enters the feasible map. This parameter curve is the material+curve. Along the material +curve (see Fig. 19), there is a match between n_m and n_s values within the feasible map, which is indicated by a green dot. This indicates that the modified mechanism satisfies the user-specifications.

The parameters of the modified mechanism can be seen in the *current state* panel and are then saved. Figure 20 shows the models of the original mechanism in the database and the modified mechanism. While the overall size of the original mechanism with material Young's modulus $E=1.5$ GPa is 180×120 mm^2 and the size of the modified mechanism is 49×32 mm^2 with material Young's modulus $E=6.7$ GPa.

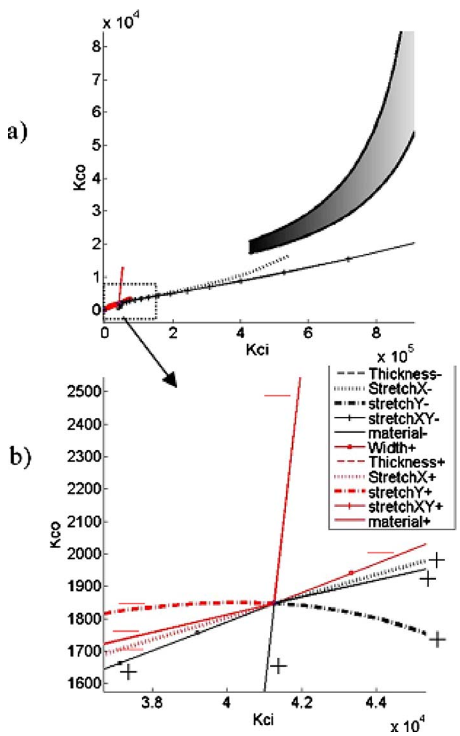

Fig. 16 Parameter curves: (*a*) the six curves represent the parameter curves from the present state and (*b*) the zoomed-in region

5 Closure

We introduced an alternate design methodology for single-input-single-output compliant mechanisms in view of practical requirements. The design is based on selection among a known set of existing compliant mechanisms. The design process is done with the help of a 2D map in conjunction with a graphical user interface. The design process is quite rapid. The design process is interactive, allowing the user to see the mechanism obeying or

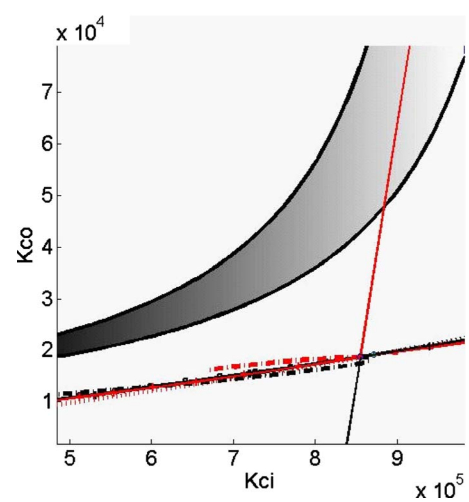

Fig. 18 Different parameter curves from the new point of design

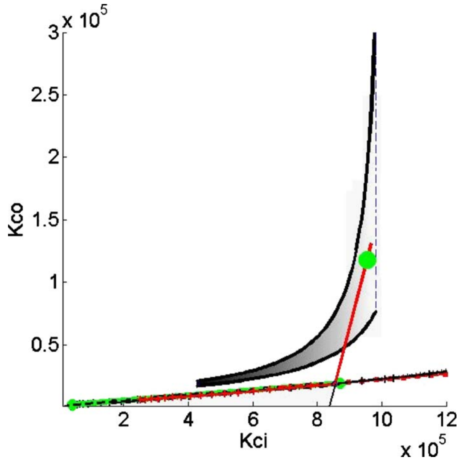

Fig. 19 The green dot indicates that there is a matching of *n* values inside the feasible map

violating his/her space constraints, manufacturing constraints, and maximum stress constraints. The method is used on a number of practical problems to design mechanisms. A detailed case-study is presented where the user-specifications are met by selecting the mechanism from a database and then modifying it. This paper includes only the basic features of the approach. Extension of the SL model to include nonlinear behavior and further development of this approach to handle other types of user-specifications is in progress.

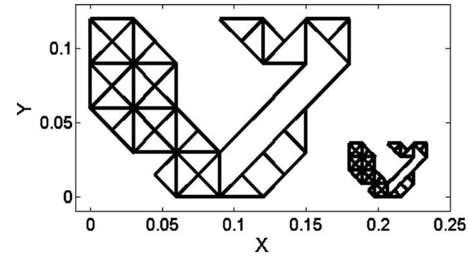

Fig. 20 The left hand side part shows the original mechanism in the database while the right hand side part shows the modified design

References

[1] Ashby, M. F., 1999, *Material Selection in Mechanical Design*, 2nd ed., Butterworth Heinemann, New York.

[2] Howell, L. L., and Midha, A., 1996, "A Loop Closure Theory for the Analysis and Synthesis of Compliant Mechanisms," ASME J. Mech. Des., **118**(1), pp. 121–125.

[3] Howell, L. L., 2001, *Compliant Mechanisms*, Wiley, New York.

[4] Frecker, M. I., Ananthasuresh, G. K., Nishiwaki, N., Kikuchi, N., and Kota, S., 1997, "Topological Synthesis of Compliant Mechanisms Using Multicriteria Optimization," ASME J. Mech. Des., **119**, pp. 238–245.

[5] Deepak, S. R., Dinesh, M., Sahu, D., and Ananthasuresh, G. K., 2008 "A Comparative Study of the Formulations and Benchmark Problems for the Topology Optimization of Compliant Mechanisms," ASME J. Mech. Rob., **1**(1), pp. 20–27.

[6] Saxena, A., 2005, "Synthesis of Compliant Mechanisms for Path Generation Using a Genetic Algorithm," ASME J. Mech. Des., **127**(4), pp. 745–752.

[7] Krishnan, G., and Ananthasuresh, G. K., 2008, "Evaluation and Design of Displacement-Amplifying Compliant Mechanisms for Sensor Applications," ASME J. Mech. Des., **130**(10), p. 102304.

[8] Wang, M. Y., 2009, "Mechanical and Geometric Advantages in Compliant Mechanism Optimization," Frontiers of Mechanical Engineering in China, **4**(3), pp. 229–241.